Visualizing 2PN Binary Black Hole Spin Precession

Alicia Lima[1,2]
Davide Gerosa[1]
[2] *Department of Physics and Astronomy, Bowdoin College, Brunswick, ME 04011, USA*
[1] *TAPIR 350-17, California Institute of Technology*
1200 E. California Boulevard, Pasadena, CA 91125, USA
(Dated: November 1, 2018)

In the post-Newtonian regime, the time it takes two black-holes to orbit each other ($t_{\rm orb}$) is much shorter than the time it takes their spins and the orbital angular momentum to precess about the direction of the total angular momentum ($t_{\rm pre}$). This, in turn, is much shorter than the time it takes the binary's orbit to shrink due to gravitational-wave emission ($t_{\rm RR}$). In short, the dynamics of precessing binary black holes is characterized by the following timescale hierarchy: $t_{\rm ort} \gg t_{\rm pre} \gg t_{\rm RR}$. This inequality has been exploited in Ref. [1], where it was shown that relative orientations of the three angular momenta on $t_{\rm pre}$ are fully specified by the magnitude of the total spin. Given the variables (ξ, J, S) identified in Ref. [1] that respect the timescale separation of the dynamics of precessing binary black holes, we build an interactive 3D visualization routine in Python to explore the phenomenology of spin precession.

I. INTRODUCTION

Before the discovery of cosmic radio waves, the Universe was studied solely through visible lights. But due to lights' strong interaction with dusty regions and Earth's atmosphere, we had a limited access to the observable universe—most of the distant astrophysical objects seen were slowly evolving stars. It was not until 1932 when Karl Jansky first discovered cosmic radio signals that we started observing pulsars, active galactic nuclei, quasars, etc. [3]. Without doubt, radio astronomy revolutionized our picture of the Universe: it revealed our Universe's violent side.

Besides seeing cosmic objects through electromagnetic waves (EM), nature has allowed us to "hear" them through gravitational waves (GWs) [2]. In 1916, Albert Einstein postulated the existence of GWs after linearizing his field equations. A century later, on September 14, 2015 the two LIGO detectors observed the first GW signal [2]. The detected signal matched the waveform predicted by General Relativity (GR) for an inpiral and merger of two black holes (BHs), where the initial BH masses are $36.2^{+5.2}_{-3.8}M_\odot$ and $29.1^{+3.7}_{-4.4}M_\odot$, resulting on a single BH of $64^{+4}_{-4}M_\odot$. Not only can we study stellar atmosphere, interstellar gas and dust using EM waves, we can also study coalescence of binary black holes (BBHs), neutron stars, and even perhaps the first fraction of a second of the big bang using GW [3].

BBH have complicated dynamics, principally when both BHs are spinning. The no-hair theorems tell us that astrophisical BHs can be completely characterized by two parameters: mass, spin. Masses enter the waveform at lower post-Newtonian (PN) order and are thus easier to infer than spins from GW data [5]. It is, therefore, very important to study the spin dynamics of BBHs system and generate more accurate templates, which in turn would improve GW parameter estimation [7]. In fact, it has been shown that templates which do not include spin effects might be poor at matching GWs coming from spinning BBHs [6]. In general, studying binary system not only allows us to enrich our astrophysical understanding of Nature, but also to test General relativity (GR). Hence, understanding the properties of binary systems from a theoretical and phenomenological point of views is crucial step to fulfill the promise of GW astronomy.

Spinning BH binaries are characterized by three angular momenta: the two spins, $\mathbf{S_1}$ and $\mathbf{S_2}$, and the orbital angular momentum, $\mathbf{L}$. On top of the binary's orbital motion, spin-spin and spin-orbit couplings make the characterization of GWs from spinning binaries more challenging [4], since they cause the three angular momenta to precess. One could reduce the complexity of the dynamics of spinning BBHs system by performing a multi-timescale analysis [1, 8]. Consider a BBH system, where r is the binary separation and M is the total mass. In the PN regime where $r \gg GM/c^2$, precessing BBHs evolve on three distinct timescales:

1. BBHs orbit each other on the orbital time $t_{\rm orb} \sim r^{3/2}/(GM)^{1/2}$;
2. The three momenta $\mathbf{S_1}$, $\mathbf{S_2}$ and $\mathbf{L}$ change direction on the precession time $t_{\rm pre} \sim c^2 r^{5/2}/(GM)^{3/2}$;
3. The orbital energy and the magnitude of the angular momentum decrease on the radiation-reaction time $t_{\rm RR} \sim c^5 r^4/(GM)^3$.

In the PN regime, the inequality below holds:

$$t_{\rm orb} \gg t_{\rm pre} \gg t_{\rm RR}. \tag{1}$$

This timescale hierarchy will be the core of the work done in this research, where we expand upon the work done in Ref [1, 8].

This report is organized as follows. In Section II we describe spin precession and its astrophysical relevance. In Section III we describe the analysis of Ref. [1], where it was shown that the relative orientations of the three

angular momentum are fully specified by a single parameter, the magnitude of the total spin, which oscillates on $t_{\rm pre}$. Solutions for generic BBH spin precession at 2PN order allow spin prcession to be classified into three morphologies. In Section IV we present our new 3D plots describing spin precession dynamics. Throughout this report, we use geometrical units ($G = c = 1$). Latin subscripts ($i = 1, 2$) label the BHs in the binary.

II. BINARY BLACK HOLE SPIN PRECESSION

A. From binary black hole spin to stellar physics

LIGO and Virgo have frequency sensitivity in the range $\sim 10 - 1000$ Hz, which means they observe the last few minutes of inspiralling stellar-mass BBHs. But in order to successfully detect the incoming GW signal and estimate the binary parameters, one needs to have accurate description of the expected waveform [7]. For a spinning BBH, the parameter space is eleven dimensional. The intrinsic parameters are: masses (2), angular momentum vector (3), and two spin vectors (6). Out of all these parameters, masses are the ones that can be extracted most accurately from the incoming GW signal, while the spins are poorly measured. One of the best spin parameter measured by LIGO and VIRGO is the effective spin ξ [12]:

$$\xi = \frac{\chi_1 \cos\theta_1 + q\chi_2 \cos\theta_2}{1+q} \tag{2}$$

where $q = m_2/m_1 \leq 1$ is the binary mass ratio, χ_1 and χ_2 are the dimensionless Kerr parameter parametrizing the spin magnitude of each BH ($S_1 = m_1^2\chi_1$, $S_2 = m_2^2\chi_2$), and θ_1 and θ_2 are the angles $\mathbf{S_1}$ and $\mathbf{S_2}$ make with $\mathbf{L}$, respectively. As evident from Eq. (1), there is a degeneracy between spin magnitudes and spin orientations in the definition of ξ.

While there are number of stellar evolution model describing the formation of BBHs system, there are still uncertainties in the spin distribution of BBHs. For instance, one of the biggest question in astrophysics is the very mechanism governing the formation of BBHs system. There are two main ways in which BBHs could be formed: the evolution of massive binary stars and capture binaries. As of today, binary parameters estimation from GW detection done by LIGO and Virgo are consistent with both formation channels (see Ref. [11] for more information on BBH formation channels).

There are a few observables which could be used to confirm or rule out formation channels such as merger rate, BH masses, BH spin magnitudes, binary eccentricities, etc.. The most promising observables are arguably the spin directions. Capture binaries systems should have no a-priori preference for any particular spin orientation, while the spins of binaries formed from the evolution of binary stars should have some correlation [7]. In order to study the expected spin direction distributions of BH binaries, one needs to coherently model spin evolution from formation to detection. This is best done by using the PN approximations. Apostolatos et *al.* [4] presented the first solutions to the orbit-averaged spin-precession equations and, later, Gerosa et *al.* [1, 8] presented solutions to precession-averaged spin dynamics equations.

B. Spin precession equation and timescale hierarchy

Consider a BH binary with mass ratio $q = m_2/m_1 \leq 1$, total mass $M = m_1 + m_2$, spins $\mathbf{S_i} = m_i^2\chi_i\hat{\mathbf{S}}_\mathbf{i}$, separation r and Newtonian angular momentum $\mathbf{L} = m_1 m_2\sqrt{r/M}\hat{\mathbf{L}}$. The merger dynamics of this system is very complex, requiring numerical simulations in order to fully solve Einstein's field equations. The early inspiral phase can be modeled by expanding Einsteins's equation in power of $\epsilon = v/c$, where v is the binary orbital velocity and c is the speed of light. This method is the so-called PN approximation, which at the core takes Newtonian description as the lowest order and GR effects as higher order perturbations [**?**]. In this framework, the instantaneous spin precession equations are (at 2PN) [12]:

$$\dot{\mathbf{S}}_\mathbf{1} = \frac{1}{2r^3}\left[(4+3q)\mathbf{L} - \frac{3qM^2\xi}{1+q}\hat{\mathbf{L}} + \mathbf{S_2}\right] \times \mathbf{S_1}, \tag{3}$$

$$\dot{\mathbf{S}}_\mathbf{2} = \frac{1}{2r^3}\left[(4+\frac{3}{q})\mathbf{L} - \frac{3M^2\xi}{1+q}\hat{\mathbf{L}} + \mathbf{S_1}\right] \times \mathbf{S_2}. \tag{4}$$

Equations (3) and (4) include both contributions due to spin-orbit interactions and contributions due to spin-spin interactions. It was shown by Apostolatos et *al.* [13] that these two interactions cause the orbital plane to precess, modulating the wave amplitude, phase and polarization. Figure (1) and Figure (2) below illustrate how spin-spin and spin-orbit couplings modulate the amplitude of the emitted GWs.

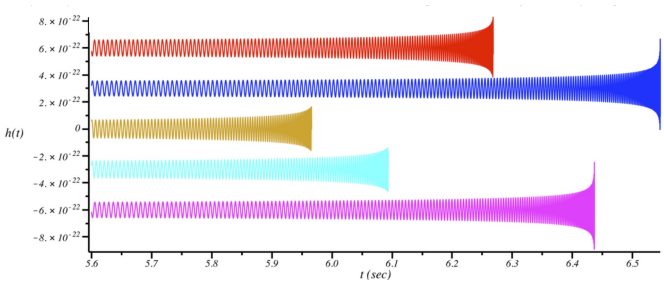

Figure 1: GW signals from inspiralling BHs with different spins. There is no precession and the spins are either aligned or anti-aligned with the orbital angular momentum. [14].

Looking at Eq. (3) and (4), one might conclude that spin precession only becomes important in the late inspiral when r is very small due to the leading r^{-3} term.

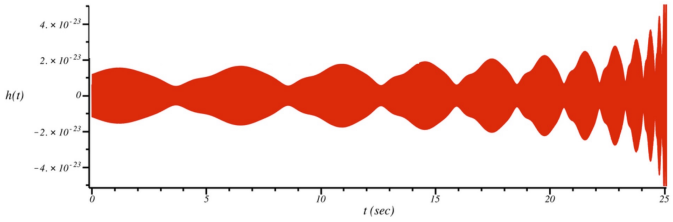

Figure 2: Precessing BBH inspiral waveform with $m_1 = 0.5M_\odot$, $m_2 = 5M_\odot$, $\chi_1 = 0$, and $\chi_2 = 0.99$. $\mathbf{S_2}$ is initially misaligned with the orbital angular momentum [14].

However, the majority of evolution occurs at large separation, hence spins generically undergo large number of cycles by the time the binary enters the merger phase.

The inequality (1) tells us that a precessing BBH completes many orbital cycle before its momenta precess, while the angular momenta complete many precession cycles before the binary separation decreases significantly. This separation of timescales is crucial to efficiently and accurately approximate the dynamics of spinning BBHs.

III. ANALYTIC SOLUTIONS ON THE PRECESSIONAL TIME SCALE

A. Reference Frame

Exploiting inequality (1) leads to a deeper understanding of the dynamics; different physical effects decouple, allowing us to analysis each process individually. The second inequality $t_{\rm pre} \ll t_{\rm RR}$ has been exploited in Ref. [1], where it was shown that relative orientations of the three angular momenta are fully specified by the magnitude of the total spin, which oscillates on the precession time. The analysis of the dynamics of spinning, precessing BBH was carried out as follow. In an inertial frame, the parameter space associated with the evolution of $\mathbf{S_1}$, $\mathbf{S_2}$ and $\mathbf{L}$ is characterized by nine variables. However, there exist several constraints on the evolution of these parameters, allowing us to reduce the number of degrees of freedom. χ_1 and χ_2 are conserved throughout the inspiral at high PN order, reducing the number of degrees of freedom from nine to seven [16]. Instead of an inertial frame, one could choose the reference frame illustrated by Fig.3 below, where one sets the x and y-component of the angular momentum $\mathbf{L}$ equal to zero, and the y-component of the spin of the first BH $\mathbf{S_1}$ equal to zero, i.e, $L_x = L_y = S_{1_y} = 0$. This reduces the number of degrees of freedom from seven to four.

At fixed separation r, in this frame only three independent coordinates are needed to describe the relative orientation of $\mathbf{S_1}$, $\mathbf{S_2}$ and $\mathbf{L}$. These can be chosen to be:

$$\cos(\theta_1) = \hat{\mathbf{S}}_\mathbf{1} \cdot \hat{\mathbf{L}}, \tag{5}$$

$$\cos(\theta_2) = \hat{\mathbf{S}}_\mathbf{2} \cdot \hat{\mathbf{L}}, \tag{6}$$

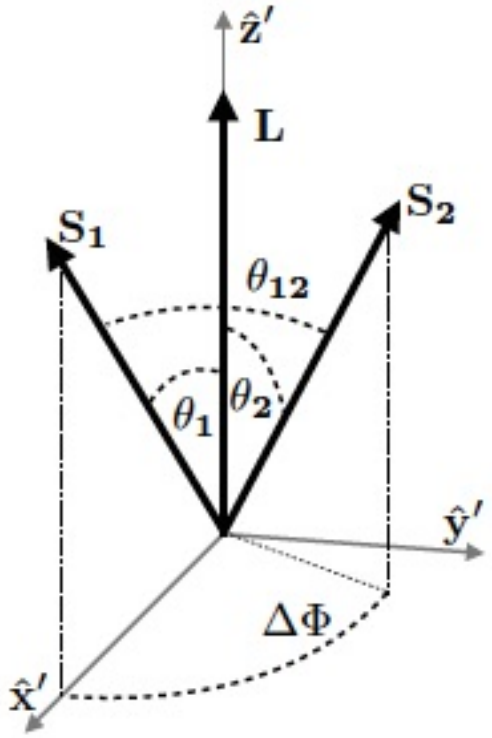

Figure 3: Reference frame used in Ref. [1] to study BBH spin precession. The angles θ_1, θ_2,θ_{12}, and $\Delta\Phi$ are defined in a framed aligned with the orbital angular momentum $\mathbf{L}$.

$$\cos(\Delta\Phi) = \frac{\hat{\mathbf{S}}_\mathbf{1} \times \hat{\mathbf{L}}}{|\hat{\mathbf{S}}_\mathbf{1} \times \hat{\mathbf{L}}|} \cdot \frac{\hat{\mathbf{S}}_\mathbf{2} \times \hat{\mathbf{L}}}{|\hat{\mathbf{S}}_\mathbf{2} \times \hat{\mathbf{L}}|}. \tag{7}$$

A more physical choice can be made to exploit the timescale separation [1]. The magnitude of the total angular momentum

$$J = |\mathbf{S_1} + \mathbf{S_2} + \mathbf{L}|. \tag{8}$$

is conserved on the timescale $t_{\rm pre}$, where GW emission can be neglected. The effective spin [12, 18]

$$\xi = M^{-2}[(1+q)\mathbf{S_1} + (1+q^{-1})\mathbf{S_2}] \cdot \mathbf{L} \tag{9}$$

is a constant according to 2PN spin-precession and 2.5PN radiation-reaction and is therefore conserved on both $t_{\rm pre}$ and $t_{\rm RR}$. The magnitude of the total spin

$$S = |\mathbf{S_1} + \mathbf{S_2}|. \tag{10}$$

oscillates within the range, $S_- \leq S \leq S_+$ on $t_{\rm pre}$.

The two descriptions, in terms of $(r, \theta_1, \theta_2, \Delta\Phi)$ and (r, ξ, J, S) are equivalent, but the latter is a somewhat nicer set of parameter since only S varies on the precession timescale. By working with (r, ξ, J, S), we have reduced the parameter space $t_{\rm pre}$ from nine dimensional to one dimensional.

B. Geometrical constraints and 2D visualization

The angles $(\theta_1, \theta_2, \Delta\Phi)$ satisfy the constraints: $\theta_1 \in [0, \pi]$, $\theta_2 \in [0, \pi]$ and $\Delta\Phi \in [-\pi, \pi]$. The others parameters, ξ, J and S also satisfy the following constraints:

$$-(1+q)(S_1 + S_2/q) \leq \xi M^2 \leq (1+q)(S_1 + S_2/q), \quad (11)$$

$$\max(L - S_1 - S_2, |S_1 - S_2| - L) \leq J \leq L + S_1 + S_2, \quad (12)$$

$$|S_1 - S_2| \leq S \leq S_1 + S_2. \quad (13)$$

It is worth stressing that these constraints are not independent of each other. For a given J, S needs to be within a specific, more restricting, range, and for a given S, ξ has a well-defined allowed region [1]. All these physical constraints can be easily calculated using PRECESSION, which is a PYTHON module describing the dynamics of precessing black-hole binaries in the Post-Newtonian regime [18].

A crucial aspect of studying the spinning binary system is visualizing and analyzing the orientation of the three angular momenta, in such a way that is both intuitive and informative. In Ref. [1], the authors showed plots in the (J, ξ) and (S, ξ) parameter space of BBHs, which provides a first partial classification of the precessional dynamics. The two plots below, Fig. 4 and Fig. 5, in the (S, ξ) and in the (J, ξ) parameter space for BBHs are created using PRECESSION.

Starting with the 2D visualization on the (S, ξ) (Fig. 4), one gains a reasonable understanding of the spin dynamics on $t_{\rm pre}$ since in this parameter space projection we suppress J. For a given J, S is allowed to take any value between S_- and S_+. For $S \in [S_-, S_+]$, one can calculate the allowed range of ξ, or more precisely, one can find the range ξ_- and ξ_+. Once we select J and ξ, the binary dynamics on $t_{\rm pre}$ is fully encoded in the evolution of S. The magnitude S oscillates between the two solutions $S_\pm$ of the equations $\xi_\pm(S) = \xi$. Figure 4 below illustrates one of effective potential loop, ξ, as a function of the total spin magnitude, S.

Besides allowing us to visualizing spin precession dynamics on t_{pre} timescale, Fig. 4 contains extra information about spin dynamics: the precessional behavior of spinning BH binaries can be classified in terms of three morphologies, depending on the evolution of $\Delta\Phi$ during a precession cycle [1]. There are three cases:

1. $\Delta\Phi$ oscillates about 0, never reaching π (blue region);
2. $\Delta\Phi$ circulates through full range $[-\pi, \pi]$ (green region);
3. $\Delta\Phi$ oscillates about π, never reaching 0 (red region).

In order to study the dynamics on the radiation-reaction timescale $t_{\rm RR}$, one needs to study the (J, ξ) parameter space for BBHs, which is illustrated in Fig.5. For a given set of q, χ_1, χ_2 and r, one finds the allowed range of J, and for each of those J one can calculate the extrema ξ_{min} and ξ_{max} of the effective potential loop in Fig. 4, which constitutes the edges of the allowed regions of Fig. 5. A binary in this plot starts from some large J value and drifts over time as the total momentum decreases because of GW emission.

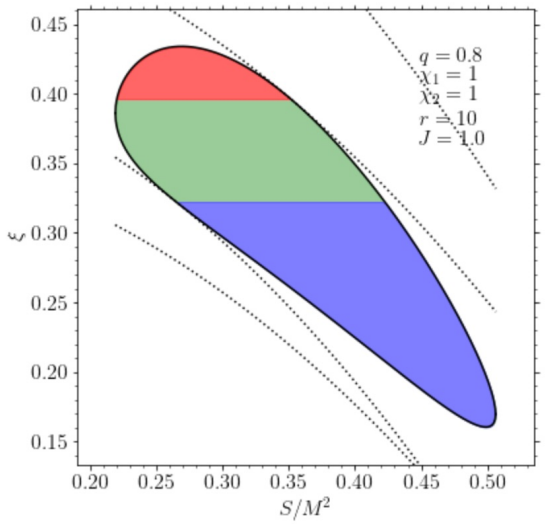

Figure 4: The (S, ξ) parameter space for BBHs. BBHs spin morphology is shown with different colors, which are determined by the behavior of $\Delta\Phi$ during a precession cycle: oscillation about 0 (blue region), circulation from $-\pi$ and π (green region), or oscillation about π (red region). Due to conservation of ξ, BBHs spins are restricted precess along horizontal lines between the turning points $S_\pm$.

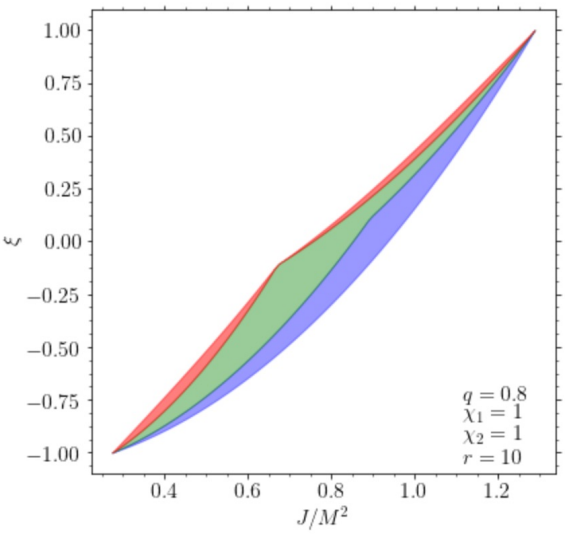

Figure 5: The (J, ξ) parameter space for BBHs for a case with $J_{\rm min} = L - S_1 - S_2$. The spin morphology is shown with different colors, as in Fig. 4. Fig. 4 can be thought of as vertical (constant J) sections of this figure.

The parameter spaces (S, ξ) and (J, ξ) allow us to separate effects on the precession timescale from those on the radiation-reaction timescale. However, they do not allow us picture the entire parameter space at the same time. After reducing the parameter-space degrees of freedom, we saw that this is a four dimensional parameter space (r, ξ, J, S). In order to understand the full phemenology of spin dynamics, one needs to construction a 3D plots that combines graphs in the $(J,\ \xi)$ and $(S,\ \xi)$ parameter space for BBHs. The dependency on r can then be introduced as time evolution.

IV. 3D VISUALIZATION IN THE (ξ, J, S) PARAMETER SPACE

We started to explore variety of 3D plot packages, principally those which are interactive in order to combine plots in the $(S,\ \xi)$, $(J,\ \xi)$ parameter spaces by using the public code PRECESSION. Various 3D plot packages were considered: Mayavi, VPython, Plotly and Matplotlib. One of the biggest challenging we faced was finding a method to interpolate over 3D surfaces. Out of all these package, Plotly was the most effective and easier to navigate. Below is an example of 3D plot we created using Plotly. For this family of BH binaries, we set $q = 0.8, \chi_1 = 1.0, \chi_2 = 1.0$ and $r = 10$.

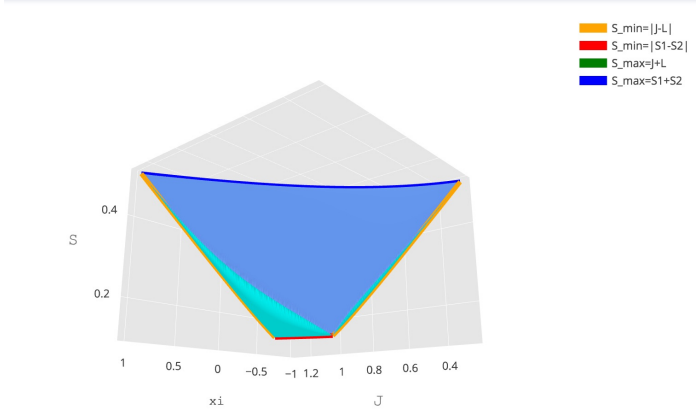

Figure 6: 3D plot of BBHs spin precession dynamics with $q = 0.8, \chi_1 = 1.0, \chi_2 = 1.0$ and $r = 10$ in the (ξ, J, S) parameter space. The edge lines, which are colored in orange, red, green and blue, correspond to the configuration where $S = S_{\rm min}$ or $S = S_{\rm max}$.The light blue and cyan surface represent all possible configuration when $S = S_+$ and $S = S_-$ respectively.

Figure 6 is the 3D plot when seen from one angle, but this can be rotated to analyze the dynamics from different angles. Figure 7 illustrates the projection of Fig. 6 on the (ξ, J).

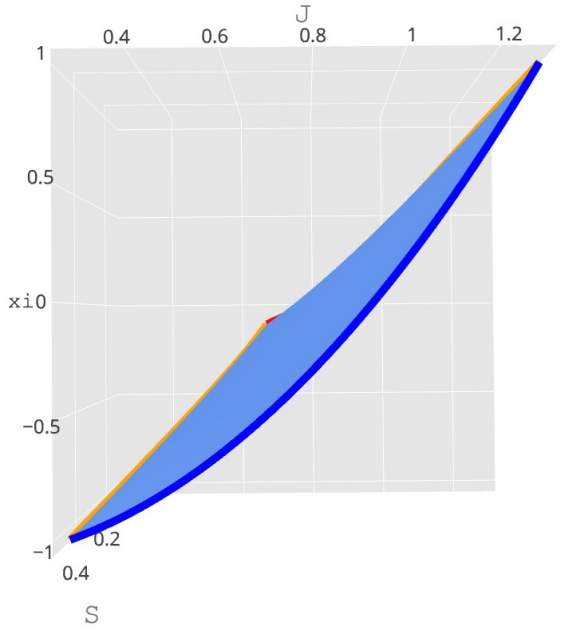

Figure 7: The same 3D plot as Figure (6), but view from different angle to highlight the (J, ξ) parameter space

Comparing Fig. 7 and Fig. 5 allows us to verify if the shape of our 3D surface is correct. If one wishes to play with the 3D plot, these tool is available at: 3D Plot (ξ, J, S) or go to the url: https://plot.ly/~alicialima/175/s-minj-l-s-mins1-s2-s-maxjl-s-maxs1s2-s-min-s-max/. With this new representation of the dynamics of BBH spin precession, we have made a further step towards better understanding of this system.

V. CONCLUSION AND FUTURE WORK

BBHs evolve on three distinct timescales: the orbital time, the precession time, and the radiation- reaction time. By exploiting this timescale hierarchy and conservation of ξ, the solution of the spin dynamics is given parametrically in terms of a single variable, the total-spin magnitude S. Furthermore, the spin precession can be classified into three distinct morphologies, which depends on the behavior of $\Delta\Phi$: oscillates about 0, oscillates about π, or circulates through the full range $[\pi, -\pi]$ over a precession cycle. Ref. [1] presents an representation of the spin dynamics in 2D parameter space, and by expanding their result, we created 3D plots, which allows us to study the full phenomenology of BBH spin precession. For future work, we will explore how to include time evolution to describe the inspiral of BBHs on the radiation-reaction timescale, which will make the 3D surface dynamical. In addition, we hope to add sliders for r, q, χ_1, χ_2, allowing us to create 3D plot for family of

binaries with different r, q, χ_1, χ_2 at the same time.

VI. ACKNOWLEDGMENTS

A.L would like to thank her mentor Dr. Gerosa for his tremendous support, as well as his help in revising this report in matters of style and content. Second, A.L. would like to thank LIGO, TAPIR, LIGO SURF, and SURF Caltech for making this research possible. Finally, A.L. would like to thank the National Society of Black Physicists (NSBP), Caltech and the Rouse family for The Carl Albert Rouse Undergraduate Research Fellowship.

The authors are grateful for the support of the US National Science Foundation's Research Experience for Undergraduates Program, award #1757303.

[1] D. Gerosa, M. Kesden, U. Sperhake, E. Berti, and R. OShaughnessy, (2015), arXiv:1506.03492 [gr-qc].
[2] B. Abbott, et al., Phys. Rev. Lett. February 2016 517/1-3 154 (2004).
[3] A. Abramovici et al. arXiv:0711.3041 [gr-qc]
[4] T. A. Apostolatos, Phys. Rev. (1994) doi:10.1103/PhysRevD.49.6274
[5] Buonanno, Alessandra, arXiv:0709.4682v1 [gr-qc]
[6] P. Grandclement, V. Kalogera, and A. Vecchio, Phys. Rev. D (2003).
[7] Schnittman, Jeremy D. Physical Review D, vol. 70, no. 12, 16 Sept. 2004, doi:10.1103/physrevd.70.124020.
[8] M. Kesden, D. Gerosa, R. O'Shaughnessy, E. Berti, U. Sperhake, arXiv:1411.0674 [gr-qc]
[9] Misner, Charles W. Gravitation. W. H Freeman and Company , 1973.
[10] B. P. Abbott et al. Phys. Rev. Lett. arXiv:1706.01812 [gr-qc]
[11] I. Mandel and A. Farmer, (2018), arXiv:1806.05820 [astro-ph.HE]
[12] Etienne Racine. Phys.Rev. arXiv:0803.1820 [gr-qc]
[13] C. Cutler, T. A. Apostolstos, L. Bildsten, L. S. Finn, E. E. Flanagan, D. Kennefick, D. M. Markovic, A. Ori, E. Poisson, G. J. Sussman, and K. S. Thorne, Phys. Rev. Lett. 70, 2984 (1993)
[14] Sounds of Spacetime, soundsofspacetime.org
[15] P. C. Peters, Phys. Rev. 136, B1224 (1964).
[16] A. Buonanno, Y. Chen, and T. Damour, Phys. Rev. D 74, 104005 (2006), gr-qc/0508067.
[17] T. Damour, PRD 64, 124013 (2001), gr-qc/0103018
[18] Gerosa, D., and Kesden, M. Physical Review D. Dec. 2017, doi:10.1103/physrevd.93.124066.
[19] L. Blanchet. Living Rev. Relativity. arXiv:1310.1528 [gr-qc]